American Mineralogist, Volume 61, pages 897–906, 1976

Experimental determination of the coherent solvus for sanidine-high albite

PHILIP J. SIPLING[1] AND RICHARD A. YUND

Department of Geological Sciences, Brown University
Providence, Rhode Island 02912

Abstract

A high sanidine was prepared by heating an adularia crystal at 1110°C. This material was subsequently exchanged in molten chlorides to produce intermediate K/Na ratios. Cleavage fragments were annealed in air between 400° and 600°C and examined by single crystal X-ray diffraction and transmission electron microscopy (TEM). The lattices of the exsolved phases are coherent across an interface approximately parallel to $(\bar{8}01)$. The reciprocal cell parameter a^* was used to determine apparent compositions of the exsolved phases, and their true compositions were obtained by correcting for the coherency strain of the lamellae. The compositions define a coherent solvus, and any pair of coexisting compositions can be determined by approaching from either a higher or lower temperature. The X-ray data from 460° to 540°C were smoothed, and the critical point of the coherent solvus was calculated to be 573°C and 37.4 mole percent $KAlSi_3O_8$. The coherent solvus lies below the strain-free solvus at all temperatures.

TEM was used to determine the position of the coherent solvus above 540°C, and the results agree well with the extrapolation of the X-ray data. The TEM results delineate the limits of exsolution, and this limit lies inside the coherent solvus below 520°C on the potassic side. This limit is believed to represent the coherent spinodal, which must coincide with the coherent solvus at its critical point. These experimental results are compared with earlier X-ray data from cryptoperthites and recent calculations of the position of the coherent solvus for alkali feldspars.

Introduction

There has been considerable emphasis in recent years on the subsolidus phase relations of the alkali feldspars with much of the experimental work directed towards determining the equilibrium or strain-free solvus. This study is concerned with the compositional relations of coherent exsolution lamellae, a feature characteristic of cryptoperthites.

Robin (1974b) and Yund (1974) have independently shown that the compositional relations of coherent cryptoperthites can be used to define a coherent solvus which lies below the strain-free solvus on a temperature–composition diagram. The compositions of the coexisting coherent lamellae are prevented from reaching the strain-free solvus because of the strain energy associated with the coherency. A general discussion of this concept and its mineralogical implications is available (Yund, 1975a), and we will assume that the reader is familiar with this concept.

In addition to recent studies of the coherent solvus, Owen and McConnell (1974) and Yund *et al.* (1974) have studied the kinetics of exsolution in the alkali feldspars with emphasis on the microstructure as determined by transmission electron microscopy (TEM). They argue that at least under certain conditions, exsolution in the alkali feldspars occurs by spinodal decomposition. The boundary of the region of spinodal decomposition on a temperature–composition diagram is the coherent spinodal. Again the reader should consult these papers or one of the summary and discussion articles (McConnell, 1975, and Yund, 1975b) for the nature and significance of these relations in mineral exsolution.

This study is based on a single crystal X-ray and TEM study of isothermally annealed samples. The purpose was to establish experimentally the position of the coherent solvus for the sanidine-high albite

[1] Present address: Department of Geology, Juniata College, Huntingdon, Pennsylvania 16652.

series. The accuracy of the location of the coherent solvus is independent of the position of the strain-free solvus and depends on the determination of apparent compositions from the reciprocal cell parameter a^* and the correction of these apparent compositions for the distortion of a^* due to coherency strain. The experimental results are compared to the theoretical calculation of the coherent solvus by Robin (1974b), to the earlier experimental results of Smith and MacKenzie (1958), and to the coherent solvus for the ordered alkali feldspars (Yund, 1974).

TEM was also used to distinguish between the coherent solvus and the coherent spinodal in this alkali feldspar series. These results are directly applicable for understanding the occurrence and determining the history of natural cryptoperthites.

Experimental procedures

The feldspar sample used for this study was prepared from crushed fragments of a natural adularia sample of about 95 mole percent $KAlSi_3O_8$ (Or_{95}) from Cristallina, Switzerland (American Museum of Natural History # 26546). The 88–125 μm fraction was annealed between 1100° and 1120°C, and the unit cell parameters determined from least-squares refinement of X-ray powder diffraction data are a = 8.581(2), b = 13.032(2), c = 7.175(2) Å and β = 116° (the numbers in parentheses are one standard deviation). The cell parameters indicate that the annealed material is a high sanidine.

Portions of this material were ion-exchanged in mixtures of molten KCl and NaCl at 1000°C for 5 days in sealed silica-glass tubes and cooled to room temperature in about one minute. The partition of alkalis between feldspar and melt was determined empirically in order to prepare the desired intermediate feldspar compositions. The compositions of the alkali ion-exchanged samples were determined using the electron probe microanalyzer. They ranged from $Or_{20.0}$ to $Or_{56.6}$. These and subsequent compositions are in mole percent on the $KAlSi_3O_8$–$NaAlSi_3O_8$ join. The calcium content was less than 0.1 mole percent An.

The exsolution experiments were done in Pt containers open to the atmosphere, and the temperatures are accurate to within ± 5°C. The extent of exsolution and the compositions of the two phases were studied using single crystal X-ray precession techniques. All crystals were mounted normal to (010) and $hk0$ photographs were taken using Zr-filtered Mo radiation.

Samples for TEM observation were prepared using either crushed grains on a carbon film or crystals mounted and thinned by ion-bombardment as described by Yund *et al.* (1974). Samples were analyzed using either a JEM-200A electron microscope operating at 200 kV or a JEM-7A operating at 100 kV.

Experimental results

Nature of the observations

A crystal of intermediate bulk composition is most suitable for determining the compositions of both exsolved phases, consequently a sample of Or_{38} was used for all experiments analyzed by single crystal X-ray techniques.

The sequence of changes observed in the precession photographs with increasing annealing time is similar to that described for the maximum microcline-low albite series (Yund, 1974), except that the samples used in this study are monoclinic and untwinned. After annealing for a few hours at 500°C, the $h00$ reflections become elongate, and with increasing time these reflections become doublets with one reflection corresponding to the sodic phase and the other to the potassic phase. Side bands were never clearly resolved on the X-ray photographs, although they were observed in the electron diffraction patterns when the lamellar spacing was less than a few hundred Å. This is similar to the results for the ordered alkali feldspars described by Yund *et al.* (1974).

Reflections from lattice planes normal to the lamellar interface show no separation on either X-ray or electron diffraction patterns, and this indicates that the lattices of the exsolved phases are perfectly coherent. The lamellar interface was determined to be about ($\bar{8}01$) from TEM micrographs. This agrees with the results of Owen and McConnell (1974) and Yund *et al.* (1974) for feldspars of nearly high and low structural state, respectively. This is also near the orientation reported for natural cryptoperthites by Laves (1952) and others.

Compositions of the exsolved phases

The values of the reciprocal cell parameter a^* were determined from X-ray diffraction single crystal photographs taken at room temperature. Orville's (1967) a^*-versus-composition data were fitted by polynomials of different order, and a third order equation was found to give an adequate fit. The compositions of the phases can be reproducibly determined from a^* to within ± 2 mole percent Or. However, an approximation for the composition of the sodic phase is necessary, due to the monoclinic to triclinic transfor-

mation in alkali feldspars with decreasing temperature. This transformation occurs in pure $NaAlSi_3O_8$ at about 980°C and in Or_{40} at about 25°C (Kroll and Bambauer, 1971). The Or_{38} sample is monoclinic at the annealing temperatures of this study, and hence when it commences to exsolve, both the sodic and potassic-rich phases are monoclinic. The sodic phase, which is less than Or_{40}, does not transform to triclinic symmetry when the exsolved crystal is cooled to room temperature because it is constrained by coherency with the potassic phase which must remain monoclinic. No evidence of triclinic symmetry was observed for the sodic phase in any experiment.

Orville's (1967) a^*-versus-composition data were measured for noncoherent phases, and hence those more sodic than about Or_{40} are triclinic. The question is whether a^* of the sodic phase is independent of its symmetry.

Grundy and Brown (1969) have studied the change in the unit cell dimensions of albite as a function of temperature. The change in the direct cell dimensions with temperature showed no discontinuities at the temperature of the triclinic to monoclinic inversion. These results suggest that there is no discontinuity in the a^*-versus-composition curve across the monoclinic to triclinic symmetry change. Thus Orville's data will be used to estimate the composition of the sodic phase even though it is constrained by the coherency to be monoclinic. We will return to the question of the validity of this assumption and the accuracy of the compositions after other pertinent results have been presented.

The compositions discussed above are referred to as apparent compositions because any arbitrary lattice spacing is distorted due to the coherency of the phases. Smith (1961) recognized this problem and suggested a correction based on the assumption that the unit cell volume is the same regardless of whether the phase is coherent or not. This method yields approximate corrections, and more rigorous methods have been described by Robin (1974b) and Tullis (1975).

The basis of Robin's (1974b) and Tullis's (1975) calculations is similar, although they do not treat the elastic constants or the compositional strains as a function of composition in the same way (Yund, 1975a). Robin's (1974b) method requires measurement of $d(\bar{2}04)$ and $d(\bar{2}01)$ which was not possible from our $hk0$ photographs. Tullis (1975) makes the correction based on apparent compositions determined from a^*, and the amount of the correction depends on the bulk composition of the crystal. Consequently, we have used only Tullis's (1975) method to correct the compositions of the exsolved phases in our experiments.

Determination of the coherent solvus using X-ray data

Eight crystals of the Or_{38} composition were annealed at different temperatures to determine the compositions of the exsolved phases. Seven of the crystals were first heated at 500°C, and the remaining crystal was first heated at 450°C for about two months, which was found sufficient to produce exsolution as discussed below. Each crystal was subsequently annealed at either a higher or lower temperature.

Above 470°C, exsolution as well as homogenization experiments were performed. For an exsolution experiment, a crystal previously annealed at a higher temperature was reannealed at a lower temperature. For a homogenization experiment, a crystal previously annealed at a lower temperature was reannealed at a higher temperature. In these experiments the compositions of the exsolved phases reached steady state, and the phases remained coherent. The results of these experiments are listed in Table 1.

The compositional change of the exsolved phases was also studied as a function of annealing time. Annealing for approximately 700 hours at 480°C was sufficient for the compositions to reach a steady state. Therefore at temperatures above 480°C even shorter annealing would be required. Single crystal X-ray methods were not useful for the determination of steady-state compositions at or above 550°C because the reflections from the sodic and potassic phases were not resolved.

The apparent compositions determined from the X-ray photographs and Orville's (1967) data for a^* were corrected for coherency strain using the data for an Or_{40} bulk composition given by Tullis (1975) in her Figure 1. The difference between this and our bulk composition is insignificant as far as these corrections are concerned. At 540°C the corrections are about 2 mole percent for both phases, and at 450°C the corrections are about 4 and 6 mole percent for the sodic and potassic phases, respectively. The true or corrected compositions are more similar (*i.e.*, less compositional difference) than the apparent compositions of the coexisting phases. The corrected compositions are shown on Figure 1, as dots for exsolution experiments and as open circles for homogenization experiments.

There is still disagreement about the location of the equilibrium or strain-free solvus for disordered alkali

TABLE 1. Compositions of the exsolved phases on the coherent solvus

T(°C)	t(hrs)	Type of experiment*	Corrected compositions Ab-rich	K-rich
550	654	Homog	----	---- +
550	659	Homog	----	---- +
540	599	Homog	30.5	54.5 +
540	722	Homog	26.5	51.5
540	957	Exsol	23.0	55.0
530	720	Homog	25.5	53.5
530	652	Exsol	23.5	54.0
520	607	Homog	24.0	55.0 +
520	434	Homog	23.5	56.0 #
520	528	Homog	24.5	55.5
520	814	Exsol	23.0	56.5
510	714	Exsol	21.0	59.0
510	672	Homog	24.5	60.0
500	1440	Exsol	22.5	56.5
500	1440	Exsol	22.5	58.0
500	1440	Exsol	22.5	58.0
500	1440	Exsol	24.0	58.0
500	1440	Exsol	23.5	57.0
500	431	Exsol	22.5	59.0
500	174	Exsol	26.0	58.5 +
500	288	Exsol	19.5	58.0 +#
500	674	Homog	24.0	59.5
490	817	Homog	21.5	60.5
490	492	Exsol	20.0	62.0
480	703	Exsol	19.5	63.0 +
480	267	Exsol	20.0	63.0 #
480	914	Exsol	20.5	61.0
480	791	Homog	19.5	64.0
470	1037	Homog	15.5	60.5 +
470	890	Exsol	18.0	67.5
450	772	Exsol	17.5	61.0 +
450	1030	Exsol	16.5	61.0 +
450	1317	Exsol	16.5	58.5 +
450	1317	Exsol	18.5	59.0 +
425	672	Exsol	16.0	68.0 +
400	672	Exsol	14.5	63.0 +

* Homog = homogenization type experiment
Exsol = exsolution type experiment
\+ not used for calculating position of coherent solvus
\# sequential to run listed above

feldspars, and the ambiguity is greatest for the potassic limb. Although we recognize that Thompson and Waldbaum's (1969b) and Waldbaum and Thompson's (1969) smoothed solvus is partially based on Luth and Tuttle's (1966) incorrect compositions, as discussed by Luth and Fenn (1973), we will use the Thompson-Waldbaum solvus for one atmosphere as representative of the approximate location of the strain-free solvus. More recent determinations of this solvus include those of Goldsmith and Newton (1974), Luth *et al.* (1974), and Smith and Parsons (1974). Smith and Parsons' data for one kbar agree with the Thompson-Waldbaum solvus to within two mole percent except below 600°C on the potassic limb. At 400°C, the Smith-Parsons solvus lies about 10 mole percent inside the Thompson-Waldbaum solvus.

The Thompson-Waldbaum solvus for one atmosphere is shown on Figure 1 as the solid curve. It is clear that the steady-state compositions of the exsolved phases, which define the coherent solvus, lie well within the strain-free solvus regardless of the exact location of the latter.

The corrected compositions have been fitted by the '*r–s*' method of Thompson and Waldbaum (1969a). The usefulness of this method has been demonstrated in several studies of Na–K solid solutions and has been shown to give results consistent with those methods relying upon the determination of the Margules parameters (Thompson and Waldbaum, 1969a, 1969b; Bachinski and Müller, 1971). The notation used is as follows:

$$s = N_\beta - N_\alpha$$

$$r = N_\beta + N_\alpha - 1$$

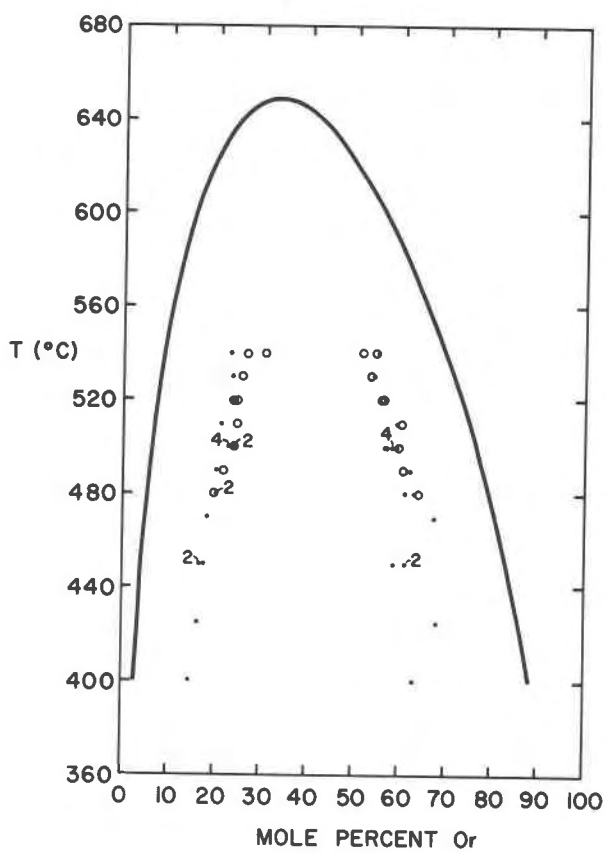

FIG. 1. Data for the coherent solvus based on single crystal X-ray diffraction and corrected for coherency strain by the method of Tullis (1975). Dots are exsolution experiments and open circles are homogenization experiments. The solid curve is the one atmosphere strain-free solvus from Waldbaum and Thompson (1969).

TABLE 2. Smoothed data for the coherent solvus

T(°C)	$N_{2\alpha}$	$N_{2\beta}$
572	0.354	0.395
570	0.338	0.413
560	0.300	0.459
550	0.279	0.490
540	0.263	0.516
530	0.250	0.539
520	0.238	0.560
510	0.228	0.579
500	0.219	0.597
490	0.210	0.614
480	0.202	0.630
470	0.195	0.646
460	0.188	0.661
450	0.181	0.676
440	0.175	0.690
430	0.168	0.703
420	0.162	0.716
410	0.156	0.729
400	0.151	0.742

where

N = mole fraction Or
β = K-rich phase
α = Na-rich phase

The functions of 'r' and 's' used in this study were ln r^2 against $1/T$ and (ath s)/s against $1/T$ where T is the temperature in K and ath = arctanh. Because the results below 470°C were somewhat inconsistent, these data points were not used in the line fitting of the aforementioned functions. For the same reasons, one point at 540°, two points at 500°, and one point at 470°C were also neglected in the data analysis. All other points were fitted by the least-squares method to a straight line weighting all points equally. The equations representing these lines are:

$$\ln r^2 = 3.88 - 5.61\ (1/T)$$

$$\frac{\text{ath}\, s}{s} = 0.45 + 0.46\ (1/T).$$

These equations were used to calculate the coherent solvus which best fits the experimental data. The calculated compositions are given in Table 2 and are represented by the lower curve on Figure 2. The critical point of the coherent solvus is at 573°C and $Or_{37.4}$.

TEM observations

TEM was used to determine the coherent solvus near the critical temperature and to attempt to distinguish the coherent spinodal at lower temperatures. This was done by observing the presence or absence of an exsolution microstructure produced in the annealed samples. The exsolution microstructure produced experimentally has been described by Owen and McConnell (1974) and Yund *et al.* (1974). We will illustrate only a typical microstructure in a sanidine-high albite crystal (Or_{41}) which was annealed at 500°C for 14 days. A bright field micrograph of a (010) section prepared by ion-bombardment is shown in Figure 3. The lamellar spacing is approximately 145 Å, and the microstructure is developed uniformly throughout the grain. The electron diffraction pattern shows two principal $h00$ reflections, indicating that the compositional difference between the lamellae is already fairly large. The change in the microstructure as a function of time is very similar to that described

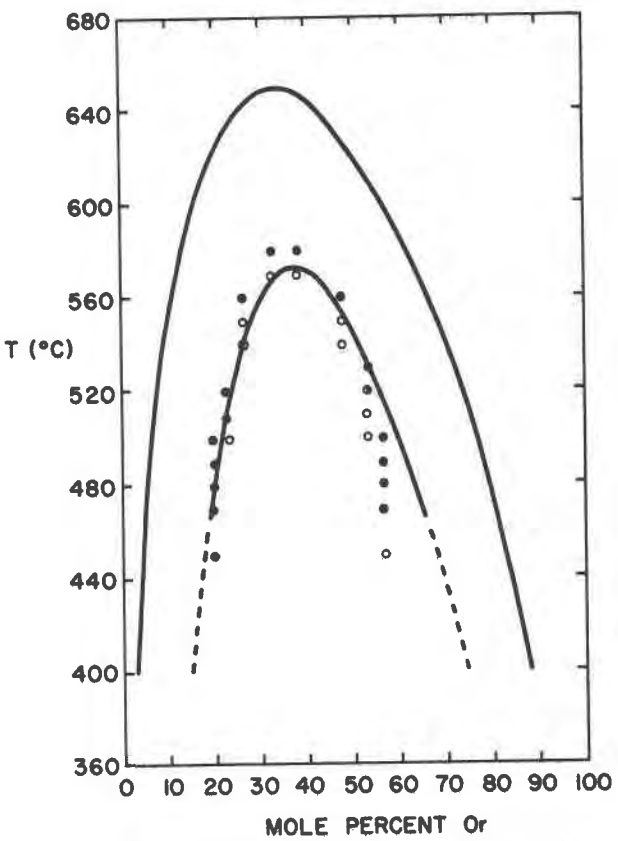

FIG. 2. The upper curve is the strain-free solvus and the lower curve is the smoothed curve for the coherent solvus based on the X-ray data. The limit of exsolution as determined by TEM is shown by the data, where open circles indicate an exsolution microstructure was observed and dots indicate no exsolution was observed. The TEM data are independent of the curve based on the X-ray data. See text.

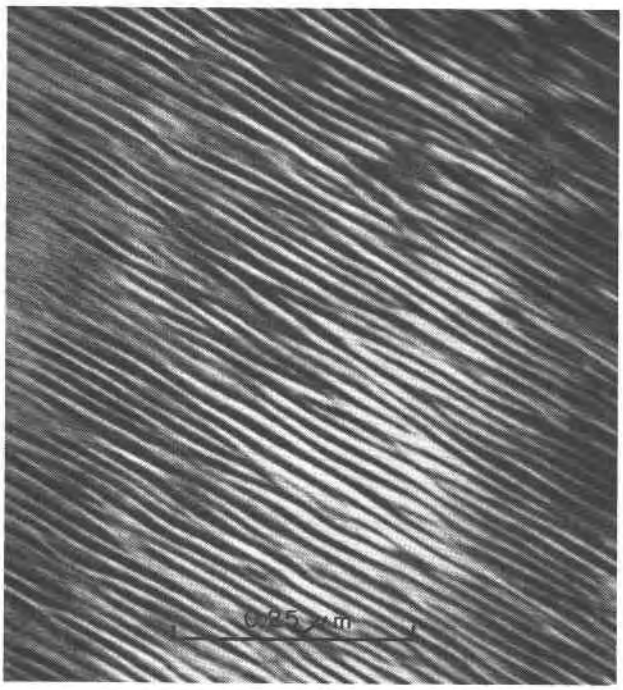

FIG. 3. Bright field micrograph of a (010) section of an Or_{41} crystal annealed at 500°C for 14 days in air. The lamellar spacing is 145 Å.

for the ordered alkali feldspars (Yund *et al.*, 1974) and will not be described in detail here.

Samples annealed just below the boundary of the region where the exsolution microstructure is observed have a larger lamellar spacing, and the contrast between the lamellae is less, because there is a smaller compositional difference, and hence the lattice spacings and their orientations are more similar in adjacent lamellae. Nevertheless, the presence or absence of an exsolution microstructure was unequivocal except in one sample which apparently had been annealed just where the temperature–compositional limit of exsolution occurs.

The results of the TEM observations are given in Table 3, and the data for temperatures above 440°C are shown on Figure 2, except for the synthetic sample (Gel) listed at the bottom of Table 3. The data for $Or_{56.6}$ indicate that below 450°C the experiments were of too short duration for the exsolution microstructure to develop. The upper curve on Figure 2 is Thompson and Waldbaum's (1969b) strain-free solvus for one atmosphere, and the lower curve is the smoothed coherent solvus based on the previous X-ray data. This curve is independent of the TEM observations.

The TEM data outline the region in which exsolution is observed, and the limit of this region defines either the coherent spinodal if spinodal decomposition is the operative exsolution mechanism, or the coherent solvus if exsolution occurs by coherent nucleation and growth. (See discussion by Yund, 1975b). At the critical point the coherent spinodal and the coherent solvus coincide (Cahn, 1962). In addition, the curves are indistinguishable within the experimental error at slightly lower temperatures. Thus the higher temperature TEM observations are here taken as defining the coherent solvus as well as the coherent spinodal. These results are in very good agreement with the coherent solvus determined from the X-ray data. These independent results demonstrate that the position of the coherent solvus is probably known to within 2–3 mole percent above 470°C.

As shown in Figure 2, if there is any distinction on

TABLE 3. Presence or absence of an exsolution microstructure as determined by transmission electron microscopy

Bulk composition	T(°C)	t(hrs)	Exsolution microstructure
$Or_{20.0}$	425	931	No
"	450	1036	No
"	470	168	No
"	480	168	No
"	490	168	No
"	500	168	No
$Or_{23.0}$	500	334	Yes
"	510	168	No
"	520	168	No
$Or_{26.8}$	540	360	Yes
"	550	360	Yes
"	560	360	No
$Or_{32.9}$	570	168	Yes
"	580	144	No
$Or_{38.3}$	570	168	Yes
"	580	144	No
$Or_{48.0}$	540	360	Yes
"	550	360	Yes
"	560	360	No
$Or_{53.0}$	500	1440	Yes
"	510	168	Yes
"	520	144	?
"	530	168	No
$Or_{56.6}$	400	1036	No
"	425	931	No
"	450	1036	Yes
"	470	168	No
"	480	168	No
"	490	168	No
"	500	168	No
Or_{38} (Gel)	560	168	Yes
"	570	168	Yes
"	580	168	No
"	590	168	No

the sodic limb between the coherent solvus and the coherent spinodal, it is quite small. However, on the potassic limb a distinction can be made. The region in which exsolution does not occur for bulk compositions within the coherent solvus is believed to represent the region between the coherent solvus and the coherent spinodal. Owen and McConnell (1974) and Yund *et al.* (1974) have presented evidence that spinodal decomposition is operative in the alkali feldspars of both low and high structural states. The data shown in Figure 2 are consistent with this interpretation.

Samples of an Or_{38} bulk composition synthesized from a gel were annealed between 560° and 590°C and examined by TEM. The results of these experiments are included in Table 3 under the heading Or_{38} (Gel). Although not shown on Figure 2, these results agree perfectly with the data shown on this figure. Because the synthetic feldspar should be completely disordered and the exsolution experiments using this sample agree with the results from the disordered and exchanged samples, the latter can be considered to be representative of totally disordered feldspars.

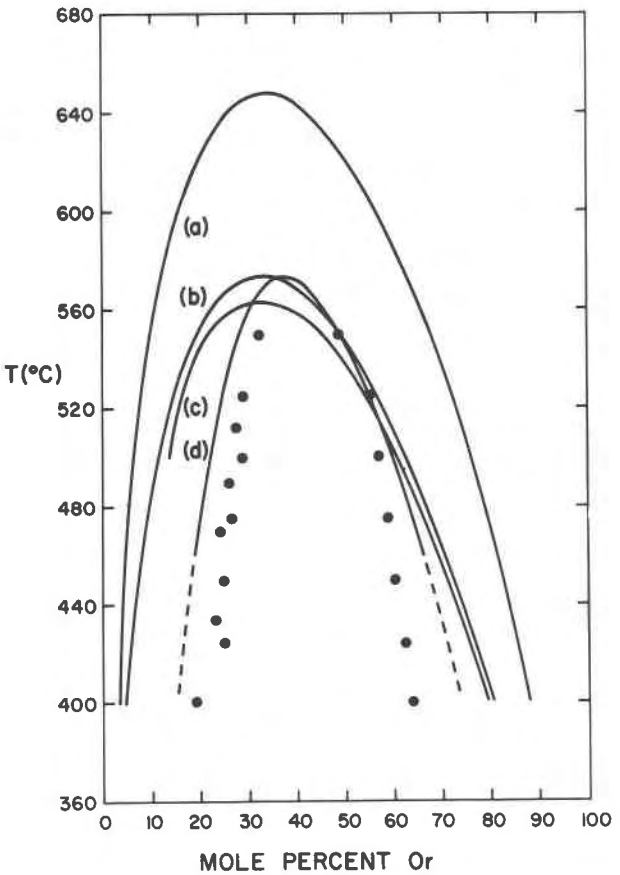

FIG. 4. Curve (a) is the strain-free solvus, curves (b) and (c) are the coherent solvi calculated by Robin (1974b) for two sets of elastic constants, and curve (d) is the coherent solvus as determined in this study. The dots on the sodic limb are the experimental data for Spencer P from Smith and MacKenzie (1958). The dots on the potassic limb are smoothed data from MacKenzie and Smith (1956) for the boundary between homogeneous and exsolved natural sanidine cryptoperthites. All data for one atmosphere.

Discussion

Robin (1974a and b) has calculated the position of the coherent solvus for the sanidine-high albite series, using an expression which he derives for the coherency strain energy and Thompson and Waldbaum's (1969b) data for the Gibbs energy as a function of composition and temperature. He uses the change in the stress-free lattice parameters of disordered alkali feldspars to calculate the strain components imposed on a lamella of composition X which exsolves coherently from a crystal of average composition X^0. From Hooke's Law he calculates the stress and remaining strain components as a function of $(X-X^0)$.

The accuracy of Robin's calculations depends on the elastic constants of alkali feldspars, the variation of their unit cell parameters with composition, and the uncertainty in the position of the strain-free solvus. He calculated the coherent solvus for 1 kbar, and we have replotted his data for 1 atmosphere on Figure 4 assuming that the pressure correction is 13.5°C/kbar (Thompson and Waldbaum, 1969b). Because of the large uncertainty in the measured elastic constants, Robin made two calculations. Curve (c) on Figure 4 corresponds to a stiffer feldspar, and curve (b) is for a more compliant feldspar.

The agreement between Robin's calculated solvi and our experimentally determined coherent solvus, curve (d) on Figure 4, is fair on the potassic limb. The overall agreement would be improved if the calculation assumed a more potassic-rich composition for the critical point and a greater compositional strain. Robin assumed a linear relation between the cell parameters and composition, and this is only approximately correct (Orville, 1967). Another uncertainty concerns the values for the elastic constants of alkali feldspars of intermediate composition. Considering the approximations in the calculations, the agreement between the calculated and experimental results is reasonable, and probably could be improved by selection of different but equally reasonable values for the calculations.

The only other data for comparison are those of Tuttle and Bowen (1958) and Smith and MacKenzie (1958). These studies determined the approximate compositional relations of the coexisting phases in cryptoperthites, although it was not recognized that these relations correspond to a coherent solvus.

Three specimens from Tuttle and Bowen's (1958) study can be used to estimate the critical point of the coherent solvus. Luth (1974) has fitted Margules parameters to these data, which consist of only three pairs of coexisting compositions for each sample. The Spencer Sparling Gulch sample gave a critical point of 537°C at Or_{43}. Spencer P and Mitchell Mesa rhyolite yield nearly identical values for the critical point, which are 576°C at Or_{35} and 577°C at Or_{37} respectively. Unfortunately Tuttle and Bowen's low-temperature data are subject to considerable error because they used $d(\bar{2}01)$ to determine compositions. Like a^*, this lattice spacing is distorted due to the coherency strain, and apparent compositions determined from this parameter are not reliable if the compositional difference of the coherent lamellae is large.

Smith and MacKenzie (1958) recognized the problem of determining compositions for cryptoperthites from $d(\bar{2}01)$. They used the reciprocal lattice angles α^* and γ^* to determine the composition of the sodic phase in Spencer P ($An_{0.5}$) as a function of temperature. Because of the coherency of the phases, the sodic phase will be constrained to be more like the monoclinic potassic phase, hence α^* and γ^* will be closer to 90° than they would if the sodic phase were not strained. This will make their compositions appear more potassic-rich than they really are.

Smith and MacKenzie's data for the sodic phase are shown by the dots on Figure 4. Their data are consistently about 7 mole percent inside our coherent solvus. In addition to the effect of the coherency strain on these compositions, other factors may contribute to this difference. The sodic phase in Spencer P is triclinic and pericline twinned. This indicates that it must be at least partially noncoherent, which would reduce the strain energy. This factor alone, however, would cause their compositions to lie outside our curve. Only seven of their experiments were for longer than 23 hours, and only two experiments were for longer than 8 days. They did not demonstrate reversibility, and the initial composition of the sodic phase was $Or_{25.5}$. Thus above approximately 460°C their experiments would have required the sodic phase to become more potassic; *i.e.*, they would have been homogenization type experiments. Their data above 460°C would be too sodic-rich and those below this temperature would be too potassic-rich if the annealing times were too short for steady state to be reached.

The dots on the potassic limb are not experimental points. They are points on the smooth curve which Smith and MacKenzie (1958) show in their Figure 4. This limb is based on the known boundary between unmixed and homogeneous natural sanidine cryptoperthites reported by MacKenzie and Smith (1956). Thus the points are actually an estimate of the coherent spinodal rather than the coherent solvus. The agreement with our coherent spinodal is surprisingly good, as seen by comparing their data shown on Figure 4 with our TEM results shown on Figure 2.

Summary and implications

The coherent solvus has been determined for disordered alkali feldspars using single-crystal X-ray diffraction data. The compositional relations of coexisting lamellae are reversible because the degree of coherency does not change. Loss of coherency would require atomic movement of the silicate framework ions whose mobilities are known to be very low at subsolvus temperatures. The largest uncertainty in the determination of the coherent solvus is associated with the compositions determined from a^*. The good agreement between the X-ray data and the independent TEM results gives us confidence that the coherent solvus is known to within 2–3 mole percent above 460°C.

The difference between the sodic limb of our coherent solvus and the data of Smith and MacKenzie (1958) may be explained by the need to correct their compositions for coherency strain. More importantly, their results demonstrate that the coherent solvus for disordered alkali feldspars is applicable to natural cryptoperthites.

Laves and Soldatos (1963) suggest the use of the term cryptoperthite for any perthite with submicroscopic lamellae. This is a useful distinction, because coarser perthites are noncoherent. Although coarse perthites may have initially formed coherently, the compositional relations of the phases are now given by the strain-free solvus. Cryptoperthites cool more rapidly and commonly remain at least partially coherent, and the compositional relations of the lamellae are given by the coherent solvus.

The coherency of cryptoperthites can be recognized from X-ray or electron diffraction patterns or by heating experiments to determine at what temperature they homogenize. For a given bulk composi-

tion, the homogenization temperature should correspond to the coherent solvus if the lamellae are highly coherent, but the temperature will be somewhat higher if the lamellae are semicoherent.

The coherency of cryptoperthites indicates that they form by exsolution from a homogeneous crystal as it cools either through the coherent solvus or the coherent spinodal. The microstructure could develop either by copious, homogeneous nucleation of coherent lamellae below the coherent solvus or by spinodal decomposition below the coherent spinodal. Owen and McConnell (1974) and Yund *et al.* (1974) have argued that spinodal unmixing is operative at least under certain conditions, and the tentative identification of the coherent spinodal in this study is consistent with this mechanism. Further work is needed to determine under what conditions in nature, if any, homogeneous nucleation between the coherent solvus and the coherent spinodal is important. Kinetic data such as those discussed by McConnell (1975) and Yund (1975b) offer the potential of proceeding to the next step of interpreting the cooling rates of cryptoperthites.

It is well known that the position of the strain-free solvus for the alkali feldspars depends on the Al and Si ordering in the tetrahedral sites (compare curves (1) and (3) on Fig. 5.). The position of the coherent solvus also depends on the structural state of the feldspar. Bachinski's data (Bachinski and Müller, 1971) for the strain-free, ordered alkali feldspar solvus are shown by curve (1) on Figure 5, and Yund's (1974) data for the coherent solvus for this series are shown as curve (2). The latter was not as carefully determined as the coherent solvus for the disordered feldspars (this study), which is shown by curve (4).

The subsolidus phase relations in the alkali feldspars are still imperfectly known, especially the order–disorder transformations. Hence it is uncertain whether feldspars from slowly cooled plutonic rocks commence to exsolve while they are still essentially disordered. Another, and perhaps more important, question is whether coarsely perthitic feldspars exsolve by the same mechanism as cryptoperthites and whether they initially develop a microstructure similar to cryptoperthites. The interpretation of coarse, noncoherent perthites depends on the answers to these and related questions.

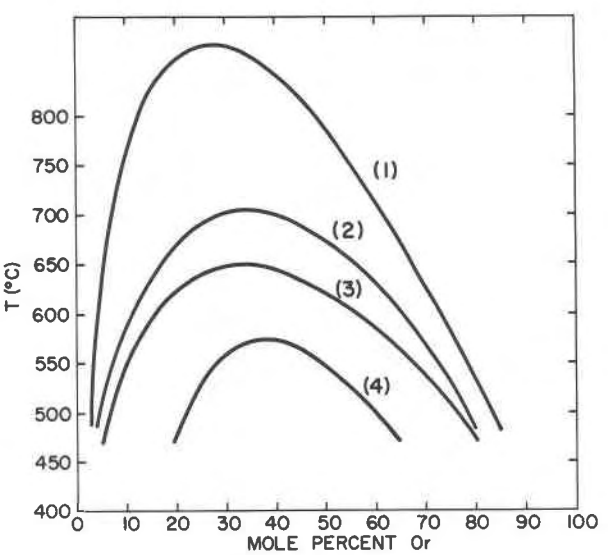

FIG. 5. Comparison of the strain-free and coherent solvi for ordered and disordered alkali feldspars. Curve (1) is the strain-free solvus (Bachinski and Müller, 1971) and (2) is the coherent solvus (Yund, 1974) for the microcline-low albite series. Curve (3) is the strain-free solvus (Waldbaum and Thompson, 1969) and (4) is the coherent solvus (this study) for sanidine-high albite. All data for one atmosphere.

Acknowledgments

We wish to thank Drs. J. Tullis and S. Kay for their helpful comments and laboratory assistance, respectively. Most of the TEM observations were made in Dr. A. C. McLaren's laboratory, Department of Physics, Monash University; this was made possible by a Fulbright Grant to one of us (RAY). The experimental work was supported by National Science Foundation Grant GA-21145.

References

BACHINSKI, S. W. AND G. MÜLLER (1971) Experimental determination of the microcline-low albite solvus. *J. Petrol.* **12,** 329–356.

CAHN, J. W. (1962) Coherent fluctuations and nucleation in isotropic solids. *Acta Met.* **10,** 907–913.

GOLDSMITH, J. R. AND R. C. NEWTON (1974) An experimental determination of the alkali feldspar solvus. In, W. S. MacKenzie and J. Zussman, Eds., *The Feldspars,* Manchester University Press. p. 337–359.

GRUNDY, H. D. AND W. L. BROWN (1969) A high-temperature X-ray study of the equilibrium forms of albite. *Mineral. Mag.* **37,** 157–172.

KROLL, H. AND H. U. BAMBAUER (1971) The displacive transformation of (K,Na,Ca)-feldspars. *Neues Jahrb. Mineral. Monatsh.* 413–416.

LAVES, F. (1952) Phase relations of the alkali feldspars. II. The stable and pseudo-stable phase relations in the alkali feldspar system. *J. Geol.* **60,** 549–574.

——— AND K. SOLDATOS (1963) Die Albit/Mikroklin-Orientierungsbeziehungen in Mikroklinperthiten und deren genetische Deutung. *Z. Kristallogr.* **118,** 69–102.

LUTH, W. C. (1974) Analysis of experimental data on alkali feldspars: unit cell parameters and solvi. In, W. S. MacKenzie and J. Zussman, Eds., *The Feldspars,* Manchester University Press. p. 249–296.

——— AND P. M. FENN (1973) Calculation of binary solvi with special reference to the sanidine-high albite solvus. *Am. Mineral.* **58,** 1009–1015.

——— AND O. F. TUTTLE (1966) The alkali feldspar solvus in the system Na_2O–K_2O–Al_2O_3–SiO_2H_2O. *Am. Mineral.* **51,** 1359–1373.

——— R. F. MARTIN AND P. M. FENN (1974) Peralkaline alkali feldspar solvi. In, W. S. MacKenzie and J. Zussman, Eds., *The Feldspars,* Manchester University Press. p. 297–312.

MACKENZIE, W. S. AND J. V. SMITH (1956) The alkali feldspars. III. An optical and X-ray study of high-temperature feldspars. *Am. Mineral.* **41,** 405–427.

MCCONNELL, J. D. C. (1975) Microstructures of minerals as petrogenetic indicators. In, F. Donath, Ed., *Annual Review of Earth and Planetary Sciences,* **3,** 129–136.

ORVILLE, P. M. (1967) Unit-cell parameters of the microcline-low albite and the sanidine-high albite solid solution series. *Am. Mineral.* **52,** 55–86.

OWEN, D. C. AND J. D. C. MCCONNELL (1974) Spinodal unmixing in an alkali feldspar. In, W. S. MacKenzie and J. Zussman, Eds., *The Feldspars,* Manchester University Press. p. 424–439.

ROBIN, P.-Y. F. (1974a) Thermodynamic equilibrium across a coherent interface in a stressed crystal. *Am. Mineral.* **59,** 1286–1298.

———(1974b) Stress and strain in cryptoperthite lamellae and the coherent solvus of alkali feldspars. *Am. Mineral.* **59,** 1299–1318.

SMITH, J. V. (1961) Explanation of strain and orientation effects in perthites. *Am. Mineral.* **46,** 1489–1493.

——— AND W. S. MACKENZIE (1958) The alkali feldspars. IV. The cooling history of high-temperature sodium-rich feldspars. *Am. Mineral.* **43,** 872–889.

SMITH, P. AND I. PARSONS (1974) The alkali-feldspar solvus at 1 kilobar water-vapour pressure. *Mineral. Mag.* **39,** 747–767.

THOMPSON, J. B., JR. AND D. R. WALDBAUM (1969a) Analysis of the two-phase region halite-sylvite in the system NaCl–KCl. *Geochim. Cosmochim. Acta,* **33,** 671–690.

——— AND D. R. WALDBAUM (1969b) Mixing properties of sanidine crystalline solutions. III. Calculations based on two-phase data. *Am. Mineral.* **54,** 811–838.

TULLIS, J. (1975) Elastic strain effects in coherent perthitic feldspars. *Contrib. Mineral. Petrol.* **49,** 83–91.

TUTTLE, O. F. AND N. L. BOWEN (1958) Origin of granite in light of experimental studies in the system $NaAlSi_3O_8$–$KAlSi_3O_8$–SiO_2–H_2O. *Geol. Soc. Am. Mem.* **74,** 153 p.

WALDBAUM, D. R. AND J. B. THOMPSON, JR. (1969) Mixing properties of sanidine crystalline solutions. IV. Phase diagrams from equations of state. *Am. Mineral.* **54,** 1274–1298.

YUND, R. A. (1974) Coherent exsolution in the alkali feldspars. In, A. W. Hofmann, B. J. Giletti, H. S. Yoder, Jr. and R. A. Yund, Eds., *Geochemical Transport and Kinetics,* Proceedings of a Carnegie Institution of Washington Symposium, June, 1973. Academic Press, New York.

———(1975a) Subsolidus phase relations in the alkali feldspars with emphasis on coherent phases. In, P. H. Ribbe, Ed., *Feldspar Mineralogy,* Mineral. Soc. Am. Short Course Notes, **2.**

———(1975b) Microstructure, kinetics, and mechanisms of alkali feldspar exsolution. In, P. H. Ribbe, Ed., *Feldspar Mineralogy,* Mineral. Soc. Am. Short Course Notes, **2.**

——— A. C. MCLAREN AND B. E. HOBBS (1974) Coarsening kinetics of the exsolution microstructure in alkali feldspars. *Contrib. Mineral. Petrol.* **48,** 45–55.

Manuscript received, September 17, 1975; accepted for publication, February 25, 1976.